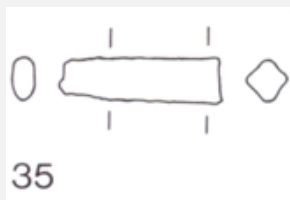


# TANG FRAGMENT OF A KNIFE HR-6246 – TIN BRONZE – LATE BRONZE AGE – SWITZERLAND

Artefact name	Tang fragment of a knife HR-6246
Authors	Marianne. Senn (EMPA, Dübendorf, Zurich, Switzerland) & Christian. Degrigny (HE-Arc CR, Neuchâtel, Neuchâtel, Switzerland)
Url	/artefacts/439/

## ≡ The object



Credit HE-Arc CR.

Fig. 1: Tin bronze tang fragment (after Rychner-Faraggi 1983, plate 35.35),

## ≡ Description and visual observation

Description of the artefact	Tang fragment with lake (shiny brown) and terrestrial (granulated green-blue) crust (Fig. 1). Dimensions: L = 2.7cm; Ø = around 5mm; WT = 5.8g.
Type of artefact	Knife
Origin	Hauterive - Champréveyres, Neuchâtel, Neuchâtel, Switzerland
Recovering date	Excavation 1983-1985, object from layer 1 (layer with material from Bronze Age till 20th cent.)
Chronology category	Late Bronze Age
chronology tpq	1050 B.C. ▼
chronology taq	800 B.C. ▼
Chronology comment	Hallstatt A/B
Burial conditions / environment	Lake
Artefact location	Laténium, Neuchâtel, Neuchâtel
Owner	Laténium, Neuchâtel, Neuchâtel
Inv. number	Hr 6246
Recorded conservation data	Not conserved

## Complementary information

Nothing to report.

Study area(s)

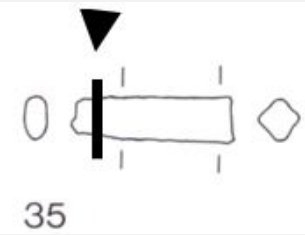


Fig. 2: Location of sampling area,

Binocular observation and representation of the corrosion structure

Stratigraphic representation: none.

MiCorr stratigraphy(ies) – Bi

Sample(s)

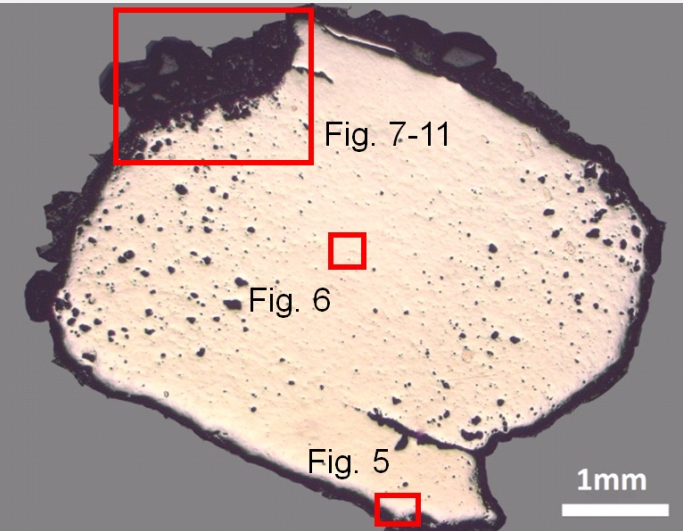


Fig. 3: Micrograph of the cross-section showing the location of Figs. 5 to 11,

Description of sample	The cross-section corresponds to a lateral cut (Fig. 2). The surface is covered with a thick corrosion crust (Fig. 3).
Alloy	Tin Bronze
Technology	Cold worked after annealing
Lab number of sample	MAH 87-197
Sample location	Musées d'art et d'histoire, Genève, Geneva
Responsible institution	Musées d'art et d'histoire, Genève, Geneva

Date and aim of sampling1987, metallography and corrosion characterisation

Complementary information

Nothing to report.

Analyses and results

Analyses performed: Metallography (etched with ferric chloride reagent), Vickers hardness testing, ICP-OES, SEM/EDS, XRD.

Non invasive analysis

Metal

The remaining metal is a tin bronze (Table 1) with high porosity and large cracks both on the left and right edges of the sample (Fig. 3). The metal contains small, elongated copper sulphide (Table 2) and Pb inclusions that are oriented parallel to the cracks. Near the metal surface, slip lines are outlined by the development of intergranular corrosion (Fig. 5). The etched metal shows small, elongated grains with slip lines (Fig. 6). Annealing is visible in areas near the surface. The average hardness of the metal is HV1 145, but significant variations are observed, depending on where the measurements are taken.

Elements	Cu	Sn	Sb	Ni	Pb	As	Ag	Co	Fe	Zn
mass%	89.85	8.02	0.60	0.55	0.34	0.34	0.18	0.10	0.02	0.01

Table 1: Chemical composition of the metal. Method of analysis: ICP-OES, Laboratory of Analytical Chemistry, Empa.

Elements	O	S	Cu	Total
mass%	0.9	20	77	98

Table 2: Chemical composition of inclusions. Method of analysis: SEM/EDS, Laboratory of Analytical Chemistry, Empa.

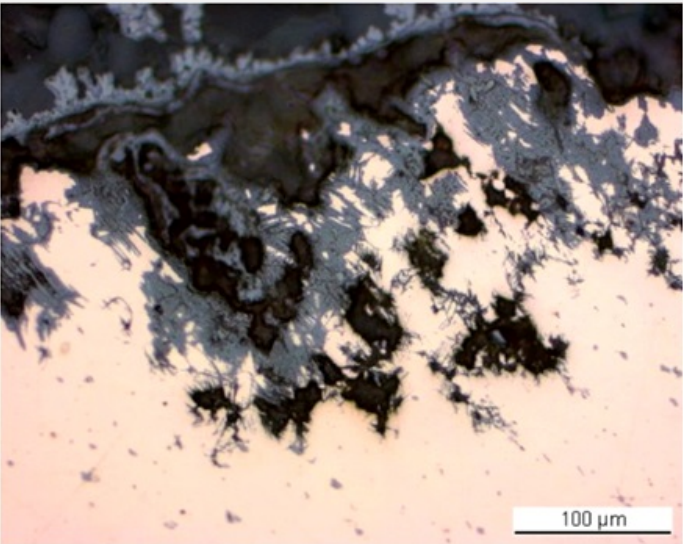


Fig. 5: Micrograph of the metal sample from Fig. 3 (inverted and reversed picture, detail), unetched, bright field. Corrosion products are in dark-grey whereas the metal is in pink. Slip lines are outlined by the development of intergranular corrosion,

Credit HE-Arc CR.

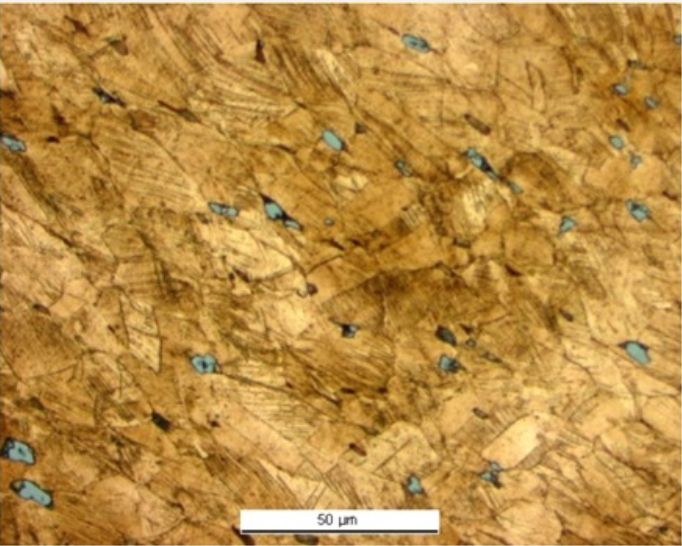


Fig. 6: Micrograph of the metal sample from Fig. 3 (detail), etched, bright field. We observe elongated grains with slip lines as well as grey copper sulphide inclusions,

Credit HE-Arc CR.

Microstructure	Elongated grains + strain lines with pores
First metal element	Cu
Other metal elements	Co, Ni, As, Ag, Sn, Sb, Pb

Complementary information

Nothing to report.

Corrosion layers

The corrosion crust has a thickness between 0.1mm and 0.7mm (Fig. 3). In bright field (Fig. 7), one can observe that the metal has been replaced by light-grey corrosion products. Adjacent to the metal is a thick, heterogeneous, dark-grey layer with a band of light-grey corrosion products. In polarised light (Fig. 8), all corrosion products which were previously light-grey appear brown-orange, the dark-grey layer turquoise. The elemental chemical distribution of the SEM images (Figs. 9 and 10) reveals that the inner corrosion products are Sn-rich whereas the adjacent band is Cu and S-rich (Fig. 11). The outer layer contains large inclusions (quartz and others, Si, Al and Na, see Figs. 10-11) and is most probably composed of malachite/ $\text{Cu}_2(\text{CO}_3)(\text{OH})_2$  (only Cu and O are detected – Fig. 11). S is distributed throughout this layer. XRD analyses indicated the presence of posnjakite/ $\text{Cu}_4\text{SO}_4(\text{OH})_6\text{H}_2\text{O}$ , chalcocite/ $\text{Cu}_2\text{S}$  and djurleite/ $\text{Cu}_{1.93}\text{S}$  (Schweizer 1994).

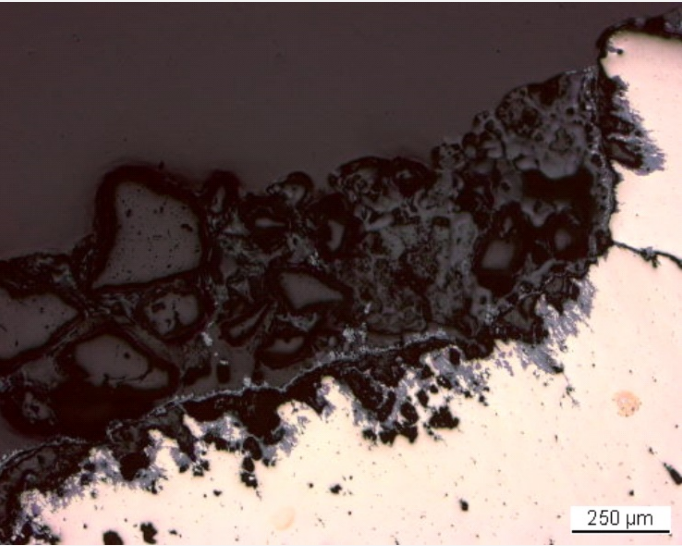
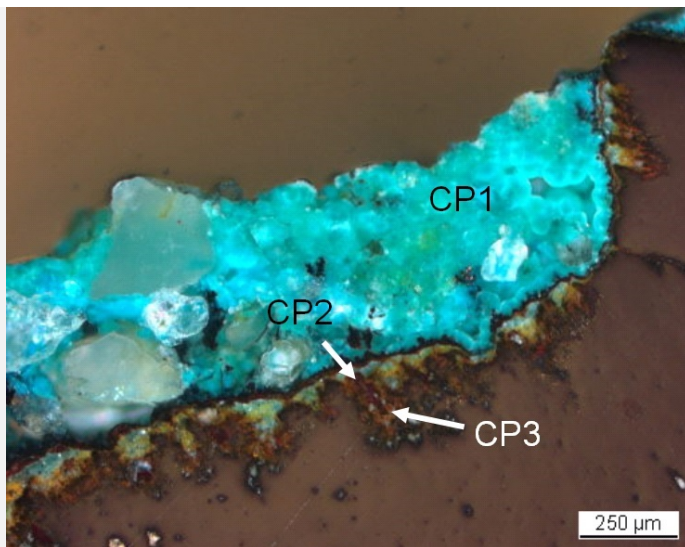


Fig. 7: Micrograph of the metal sample from Fig. 3 (detail), unetched, bright field. The inner light-grey corrosion products extend into the metal surface (in pink) and appear as a line within the dark-grey corrosion layer,

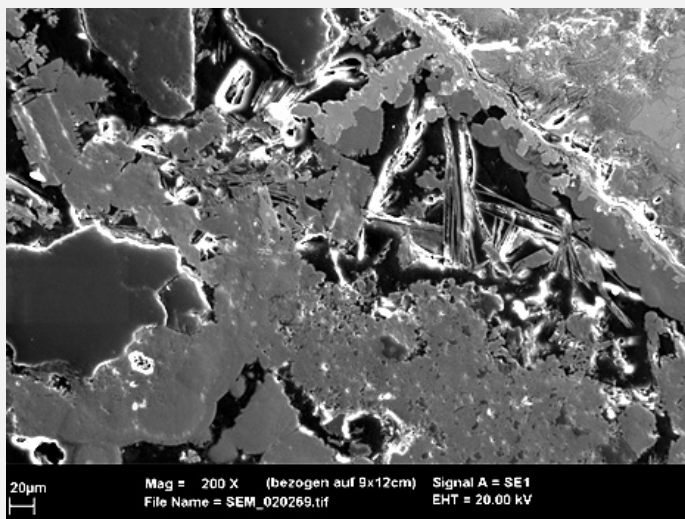
Credit HE-Arc CR.





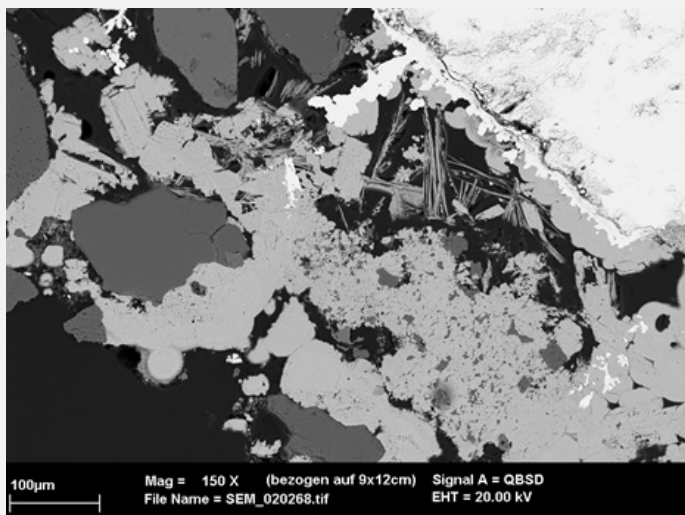
Credit HE-Arc CR.

Fig. 8: Micrograph similar to Fig. 7 and corresponding to the stratigraphy of Fig. 4, polarized light. One can see that large mineral features are incorporated only in the corrosion layers above the brown-orange corrosion band,



Credit HE-Arc CR.

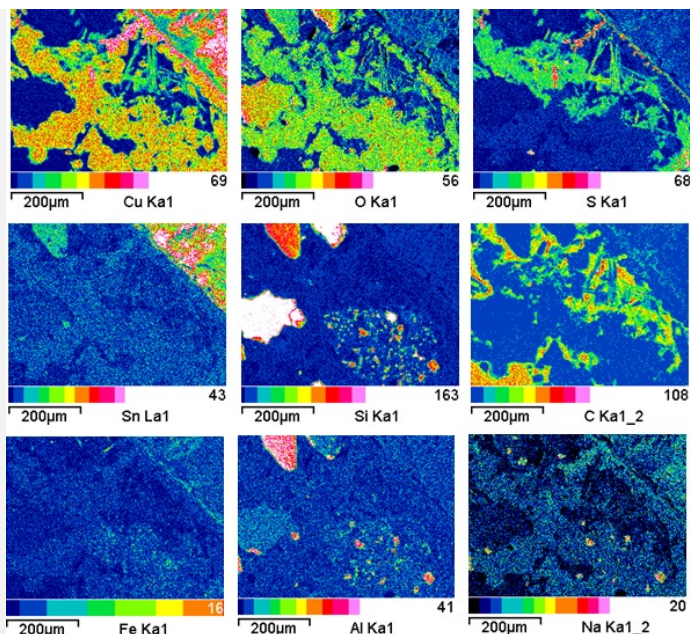
Fig. 9: SEM image (detail of Fig. 7), SE-mode. From bottom to top right: the thick, porous outer corrosion layer, the light-grey band and the remaining metal,



Credit HE-Arc CR.

Fig. 10: SEM image, similar to Fig. 9, BSE-mode,

Fig. 11: EDS elemental chemical distribution of the SEM image of Fig. 9. Method of examination: SEM/EDS, Laboratory of Analytical Chemistry, Empa,



Credit Empa.

**Corrosion form** Uniform - transgranular

**Corrosion type** Type I (Robbiola)

#### Complementary information

Nothing to report.

#### ✧ MiCorr stratigraphy(ies) – CS

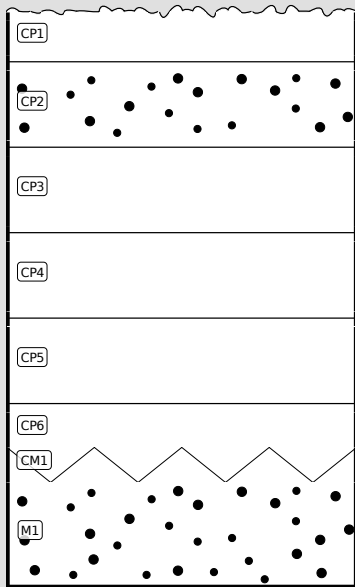


Fig. 4: Stratigraphic representation of the object in cross-section using the MiCorr application. The characteristics of the strata are only accessible by clicking on the drawing that redirects you to the search tool by stratigraphy representation. This representation can be compared to Fig. 8, Credit HE-Arc CR.

#### ✧ Synthesis of the binocular / cross-section examination of the corrosion structure

Corrected stratigraphic representation: none.

## ✧ Conclusion

The tang fragment is made from a leaded bronze and has been cold worked on the top surface after annealing. The SEM/EDX examination and past XRD analyses indicate the presence of chalcopryite in the corrosion crust, typical of lake context (Schweizer 1994), enriched with Sn close to the metal surface and depleted of Cu on the outer surface. This object was certainly abandoned rather quickly in an anaerobic, humid and S and Fe-rich environment, favouring then the formation of chalcopryite. The limit of the original surface most probably lies between the Sn-rich inner layer and the Fe and S-rich outer layers. The presence of iron oxides on top of the copper corrosion crust has not yet been explained. The corrosion is a type 1 according Robbiola et al. 1998.

## ✧ References

### *References on object and sample*

#### **References object**

1. Rychner-Faraggi A-M. (1993) Hauterive – Champréveyres 9. Métal et parure au Bronze final. Archéologie neuchâteloise, 17 (Neuchâtel).

#### **References sample**

2. Rapport d'examen, Laboratoire Musées d'art et d'histoire, Geneva GE (1987), 87-194 à 197

3. Schweizer, F. (1994) Objets en bronze provenant de sites lacustre: de leur patine à leur biographie. In: L'œuvre d'art sous le regard des sciences (éd. Rinuy, A. and Schweizer, F.), 143-157.

### *References on analytic methods and interpretation*

4. Robbiola, L., Blengino, J-M., Fiaud, C. (1998) Morphology and mechanisms of formation of natural patinas on archaeological Cu-Sn alloys, Corrosion Science, 40, 12, 2083-2111.